Dynamic profiling of protein mole synthesis rates during C2C12 myoblast differentiation.

Running title: Protein synthesis during myoblast differentiation

Ben N. Stansfield*, Alexander D. Brown*, Claire E. Stewart, and Jatin G. Burniston†.

Research Institute for Sport & Exercise Sciences, Liverpool John Moores University, Liverpool, UK.

*These authors contributed equally to the work.

†Address for Correspondence: Jatin G Burniston PhD FECSS

Professor of Muscle Proteomics

Research Institute for Sport & Exercise Sciences (RISES)

Liverpool Centre for Cardiovascular Science (LCCS)

Liverpool John Moores University,

Tom Reilly Building, Byrom Street,

Liverpool, L3 3AF,

United Kingdom.

Tel: +44 (0) 151 904 6265

Email: j.burniston@ljmu.ac.uk

Keywords:

Deuterium oxide; Fractional synthesis rate; Mass spectrometry; Protein synthesis; Stable isotope

Word Count

5079 including references and figure legends

Abstract

Mole (MSR) and fractional (FSR) synthesis rates of proteins during C2C12 myoblast differentiation were investigated. Myoblast cultures supplemented with D_2O during 0-24 h or 72-96 h of differentiation were analysed by LC-MS/MS to calculate protein FSR and MSR after samples were spiked with yeast alcohol dehydrogenase (ADH1). Profiling of 153 proteins detected 70 significant ($p \leq 0.05$, FDR ≤1 %) differences in abundance between cell states. Early differentiation was enriched by clusters of ribosomal and heat shock proteins, whereas later differentiation was associated with actin filament binding. The median (first - third quartile) FSR (%/h) during early differentiation 4.1 (2.7-5.3) was ~2-fold greater than later differentiation 1.7 (1.0-2.2), equating to MSR of 0.64, (0.38-1.2) and 0.28, (0.1-0.5) fmol/h/ug total protein, respectively. MSR corresponded more closely with abundance data and highlighted proteins associated with glycolytic processes and intermediate filament protein binding that were not evident amongst FSR data. Similarly, MSR during early differentiation accounted for 78 % of the variation in protein abundance during later differentiation, whereas FSR accounted for 4%. Conclusively, the interpretation of protein synthesis data differed when reported in mole or fractional terms, which has consequences when studying the allocation of cellular resources.

Statement of Significance

Fractional protein synthesis measurements may be confounded when studying systems undergoing changes in protein abundance. To address this issue, we further developed our dynamic proteome profiling (DPP) method to include protein abundance (ABD) data measured in mole units against a spiked-in standard (yeast alcohol dehydrogenase 1). When combined with fractional synthesis rates, measured by mass isotopomer analysis, ABD data enable the calculation of mole synthesis rates (MSR) on a protein-by-protein basis. During C2C12 differentiation MSR and FSR data gave rise to different biological interpretations. MSR measurements during early differentiation prediction subsequent changes in protein abundance better than FSR and exhibited a stronger relationship with published changes in RNA.

1. Introduction

Muscle primarily consists of multinucleated myofibers, that originate from myogenic precursors through a program of differentiation during embryonic development [1]. Myogenic differentiation is also reactivated during regeneration in adult muscle, in response to injury or during periods of adaptation to exercise [2]. The differentiation of myogenic precursors involves complex temporal patterns of gene expression[3] and cell cycle regulation [4]. However, differentiation also involves substantial changes to the myocyte proteome [5] and during differentiation myoblasts fuse and hypertrophy, which may be accompanied by changes to the synthesis of individual proteins. Targeted analyses [6] report the synthesis of contractile proteins coincides with myoblast fusion but wider-spread changes in protein abundance occur during the differentiation program [5] [7], including changes to proteins specifically involved in ribosomal translation[8].

Stable isotope labelling of amino acids in cell culture (SILAC), has allowed for measurements of individual protein fractional synthesis rates (FSR) in C2C12 myotubes [9]. More recently deuterium oxide (D_2O) labelling has been adopted to investigate mixed protein FSR in C2C12 myoblasts and myotubes [10, 11]. We have studied protein-specific FSR in rat [12, 13] and human [14] [15] muscle using D_2O *in vivo* and dynamic proteome profiling (DPP) [16] to study both the relative abundance and FSR of individual proteins. However, FSR data are fractional measurements of an unknown whole, i.e. protein abundance. Therefore, the interpretation of FSR may be confounded when used to study changes in cell state underpinned by marked changes in protein abundance [5]. Co-occurring changes in protein abundance may need to be incorporated with synthesis data to gain an accurate interpretation biological processes [17] [18]. Herein we report a development of our DPP method to provide synthesis and data in mole (e.g. fmol/h/ug total protein) units. Importantly, the biological interpretation of our current data is different when expressed in mole rather than fractional terms, and our data expressed in mole units gave a better prediction of subsequent changes in protein abundance.

2. Materials and Methods

2.1 Cell Culture

C2C12 murine myoblasts (ATCC; Rockville, MD, USA) were resuscitated from liquid nitrogen and seeded onto gelatinised T75 flasks (Nunc, Roskilde, Denmark) at 1 x 10^6 cells/ml in growth medium (GM) containing: Dulbecco's Modified Eagle Medium (DMEM), 10 % heat-inactivated fetal bovine serum (FBS), 10 % heat-inactivated new-born calf serum, 2 mM L-glutamine, and 1 % penicillin-streptomycin. Cells were incubated in 5 % CO_2 at 37 °C (HERAcell 150i incubator; Thermo Scientific) until 80 % confluent and then reseeded at 100,000 cells/ml on gelatinised 6-well plates (Nunc, Roskilde, Denmark).

Upon attaining 80 % confluency, cells were washed twice in phosphate buffered saline (PBS; 10 mM phosphate buffer, 2.7 mM KCL, 137 mM NaCl, pH 7.4; Sigma-Aldrich, Dorset, UK) and incubated in 2 ml differentiation medium (DM) containing: DMEM, 2 % heat-inactivated horse serum, 2 mM L-glutamine, 1 % penicillin-streptomycin. Isotopic labelling of newly synthesised proteins was achieved by supplementing DM with sterilised 99.8 % D_2O (Sigma-Aldrich, Dorset, UK). To investigate protein FSR during early differentiation, separate cultures of cells were incubated in DM containing either H_2O or D_2O during 0 h – 24 h of differentiation. Similarly, protein FSR during late differentiation was investigated in separate cell cultures incubated in DM containing either H_2O or D_2O during 72 h – 96 h of differentiation. Proteins extracted from control (DM + H_2O) cells were used to measure the natural isotopic abundance of proteins in the absence of D_2O. Cell photomicrographs were acquired after 0 h and 96 h of culture in DM (Figure 1) and analysed using Image J software (IBIDI, Munich, Germany). Myotubes were classified as cells that contained 3 or more myonuclei/tube. Myotube length (µm) was measured along the long axis of each myotube, diameter (µm) was averaged from measurements at three equidistant positions, and myotube area (µm^2) was calculated by drawing manually around the sarcolemma.

2.2 Proteomic analysis

Cells were washed twice with ice cold PBS, prior to incubation on ice in 250 µl/well RIPA buffer (0.5 M Tris-HCL, pH 7.4, 1.5 M NaCl, 2.5 % deoxycholic acid, 10 % NP-40, 10 mM EDTA) for 5 min. Cells were then harvested using a cell scraper and stored at –80 °C. The protein concentration of harvested samples was measured using a bicinchoninic acid (BCA™) protein assay (Pierce, Rockford, IL) against bovine serum albumin (BSA) standards (0-2 mg/ml) prepared in RIPA buffer. Proteins were digested consistent with our recent work [13-15]. Briefly, lysates containing 100 µg protein were digested with trypsin using the filter aided sample preparation (FASP) method. Aliquots, containing 4 µg peptides, were desalted using C_{18} Zip-tips (Millipore, Billercia, MA, USA) and resuspended in 0.1 % formic acid spiked with 10 fmol/ul yeast alcohol dehydrogenase (ADH1) (Waters Corp. Milford, MA) in preparation for liquid chromatography-mass spectrometry (LC-MS/MS) analysis.

Peptide mixtures were analysed by nanoscale reverse-phase ultra-performance liquid chromatography (UPLC; NanoAcquity; Waters Corp.) and online electrospray ionization quadrupole–time-of flight mass spectrometry (Q-TOF Premier; Waters Corp.), as previously reported [13-15]. For all measurements, the mass spectrometer was operated in positive electrospray ionization mode at a resolution of >10,000 full width at half maximum (FWHM). Peptide mass spectra were recorded between 350 and 1600 m/z using survey scans of 0.9 s duration with an interscan delay of 0.1 s. In addition, data-dependent MS/MS spectra were collected from control samples over the range 50–2000 m/z for the 5 most abundant precursor ions of charge 2+ or 3+. The mass spectrometry proteomics data have been deposited to ProteomeXchange (http://www.proteomexchange.org), dataset identifier PXD021125.

2.3 Label-free quantitation of protein abundance

Label-free quantitation was performed using Progenesis Quantitative Informatics for proteomics (Nonlinear Dynamics, Newcastle, UK) consistent with our previous work [13, 14, 19]. MS/MS spectra were exported in Mascot generic format and searched against the Swiss-Prot database restricted to ‘mus

musculus' (17,006 sequences) using a locally implemented Mascot (www.matrixscience.com) server (version 2.2.03). The enzyme specificity was trypsin allowing 1 missed cleavage, carbamidomethyl modification of cysteine (fixed), deamidation of asparagine and glutamine (variable), oxidation of methionine (variable) and an m/z error of ± 0.3 Da. The Mascot output (xml format), restricted to non-homologous protein identifications was recombined with MS profile data in Progenesis. For statistical analysis, log-transformed MS data were normalized by inter-sample abundance ratio, and differences in relative protein abundance were investigated using nonconflicting peptides only. In addition, data were normalised to yeast ADH1 to estimate protein abundances in fmol/µg protein using the Hi-N method [20].

2.4 Calculation of protein synthesis rates

Peptide mass isotopomer abundance data were extracted from MS only spectra using Progenesis Quantitative Informatics (Nonlinear Dynamics, Newcastle, UK). Consistent with our previous work [13-15], the abundances of the monoisotopic peak (m_0), m_1, m_2 and m_3 mass isotopomers were collected over the entire chromatographic peak for each non-conflicting peptide that was used for label-free quantitation. Peptides that were not resolved to at least 4 mass isotopomers (m_{0-3}) were excluded.

Precursor enrichment was back calculated from peptide mass isotopomer data according to [12, 21]. Briefly the enriched molar fraction of each mass isotopomer was calculated by subtracting the molar fraction of the unlabelled control peptide from the equivalent D_2O-labelled peptide and the enrichment ratio between m_2 and m_1 mass isotopomers was used to calculate precursor enrichment (p) using equation 1.

$$p = \left(\left(\frac{EM_2}{EM_1}\right)\Big/\frac{(n-1)}{2}\right)\cdot 100 \qquad \text{(Equation 1)}$$

Where EM_1 is the enriched molar fraction of m_1 and EM_2 is the enriched molar fraction of m_2 and n is the number of H-D exchange sites counted by referencing the peptide amino acid sequence against standard tables [22].

Incorporation of deuterium into newly synthesized protein results in a decrease in the molar fraction (fm_0) of the monoisotopic (m_0) peak that follows the pattern of an exponential decay. The rate constant (*k)* for the decay of fm_0 was calculated as a first-order exponential spanning from the beginning (*t0*) to end (*t*) of the 24 h D_2O labelling period.

$$k = \frac{1}{t - t0} \bullet -\ln\left(\frac{fm_{0_t}}{fm_{0_{t0}}}\right)$$

(Equation 2)

The rate of change, *k,* is a function of the number (*n*) of ^2H exchangeable H—C bonds, and this was accounted for by referencing each peptide sequence against standard tables [22]. FSR, was derived by dividing *k* by the molar percent enrichment of deuterium in the precursor (*p*) pool. Protein FSR was reported as the median of peptide values assigned to each protein (decimal values were multiplied by 100 to give FSR in (%/h). Protein half-life ($t_{1/2}$) in h was estimated from decimal FSR data by Equation 3:

$$t_2^1 = \frac{ln2}{\left(\frac{FSR}{100}\right)}$$

(Equation 3)

Mole synthesis rate (MSR) was calculated by multiplying protein FSR expressed as a decimal by the protein abundance normalised to the 50 fmol yeast ADH1 spike-in[20].

2.5 Statistical analysis

Statistical analyses were performed in R Studio version 3.6.2. Data are presented as mean ± SD unless otherwise stated. Morphological analysis of control and labelled myotubes after 96 h differentiation was conducted using independent t-tests. Data collected from cell cultures harvested at 0 h and 24 h

(control and labelled) of differentiation were used to quantify protein abundances (n = 3) during early differentiation. Similarly, control and labelled cultures harvested at 72 h and 96 h were used to provide abundance measurements (n=3) during later differentiation. Differences in protein abundance between early and later differentiation were investigated by ANOVA. Statistical significance was set at $p \leq 0.05$ and FDR was set at 1 % based on q values [23]. Data from each H2O (control) and D2O labelled sample were used to calculate protein FSR and MSR during early (24 h) or late (96 h) differentiation.

2.6 Bioinformatics

2D enrichment analysis [24] was conducted against published [25] transcriptome data, using the Perseus platform [26], with significance being set at $p \leq 0.02$. Protein interactions were investigating using bibliometric mining in the search tool for the retrieval of interacting genes/proteins (STRING; http://string-db.org/) [27].

3. Results and Discussion

Supplementation of DM with D_2O had no observable effect on myocyte differentiation (Figure 1B and C). There were equivalent numbers of myotubes in n=3 fields of view in control (14 ± 3) and deuterium-labelled (13 ± 3) cells. Myotube length (60.03 ± 22.51 µm) and diameter (6.5 ± 2.37 µm) in deuterium-labelled cultures was not different from the length (59.53 ± 24.88 µm) and diameter (6.03 ± 1.99 µm) of myotubes grown in control DM (Figure 1D-F). As expected, the distribution of peptide mass isotopomers was similar between samples harvested prior to (Figure 1G) and after (Figure 1H) 24 h incubation in control DM, whereas cells grown in DM supplemented with D_2O exhibited robust changes in isotopomer distribution and a decrease in the fraction (fm_0) of the peptide monoisotopic (m_0) peak (Figure 1I).

Label free quantitation included 3546 peptides from 153 proteins that had at least one unique peptide detected in each sample during both early and later periods of differentiation. Ten proteins (n = 12 peptides) were not identified in all samples and were disregarded. The complete list of protein abundance and synthesis data is provided in Supplementary Table 1. Seventy proteins exhibited statistically significant ($P \leq 0.05$, FDR ≤ 1%) differences in abundance between early and late differentiation (Figure 2A), including 27 proteins that increased and 43 proteins that decreased in abundance. Our current profiling of abundance data add to earlier analyses of C2C12 myoblast differentiation using 2-D gel electrophoresis [7] and LC-MS/MS [5]. In agreement with earlier reports [5], ribosomal proteins and eukaryotic initiation factors were enriched in C2C12 myoblasts. In addition, proteins associated with chromatin regulation (e.g. nucleosome assembly protein; NAP1L1;[28]), cell proliferation (e.g. prothymosin alpha; PTMA [29]) and protein folding (e.g. peptidyl-prolyl cis-trans isomerase A ;PPIA [30]) were significantly greater in abundance during early differentiation (Figure 2A). Heat shock proteins are integral to protein translation and prevent misfolding during elongation or assist in the correct folding of polypeptides after termination [31]. Isoforms of HS90 (HS90A, HS90B) maintain proteostasis by facilitating the degradation of unfolded or redundant proteins [32]. We report

200 significantly greater abundance of each HS90 isoform during early differentiation, alongside
201 mitochondrial heat shock protein (CH60) that facilitates the correct folding of proteins imported to the
202 mitochondrial matrix [33]. These findings provide the first protein confirmation of transcriptome analysis
203 [34], reporting differential expression of HSP genes during the differentiation of mouse primary
204 myoblasts.

205 2D Enrichment analysis (Figure 2B) demonstrated that differentiation was associated with significant
206 enrichment of cytoskeletal components and actin filament-based processes that were not reflected at
207 the transcriptome level. Conversely, the transcriptome data highlighted the enrichment of biosynthetic
208 process during differentiation, which were not faithfully replicated at the proteome level. The
209 disparities between RNAseq and proteome data may relate to differences in sampling time (4 d in the
210 current proteomic work and 7 d in the published [25] RNAseq analysis) or may suggest regulation by
211 processes in addition to transcription. Indeed, the correlation between protein abundance changes and
212 published [25] RNAseq differences at 24 h and 7 days of differentiation was r^2=0.3275 (Figure 2C), which
213 is similar to past publications [35].

214 Changes in protein abundance are ultimately underpinned by the balance between protein synthesis
215 and protein degradation. Protein FSR was calculated for 115 of the 153 proteins that had clearly
216 resolved mass isotopomer envelopes in both labelled and unlabelled samples. The median FSR of
217 proteins early during differentiation (4.11, IQR = 2.70-5.31 %/h) was ~2 fold greater than the median
218 FSR (1.70, IQR = 0.97-2.16 %/h) later during differentiation. These FSR values equate to a median half-
219 life ($t_{1/2}$) of 16.9 h and 44.4 h during early and late differentiation, respectively. Cell cycle arrest occurs
220 rapidly after myoblasts are transferred to DM [36] and the marked decrease in protein turnover is
221 consistent with the significant reduction in the abundance of ribosomal proteins (Figure 2A). Notably,
222 the average half-life of proteins during 72 – 96 h of differentiation in C2C12 (0.9 ± 0.6 d) was
223 substantially shorter than their corresponding half-life's in young mouse EDL (22.5 ± 17.2 d) or soleus
224 muscle in vivo (16.6 ± 8.8 d). There was also no relationship (r^2 < 0.03) amongst 32 proteins that were
225 matched in the current work with FSR reported in mouse fast- and slow-twitch muscle in vivo [39]. These

findings are consistent with [40] and raise challenges for the integration of data across cell and animal models. Our calculations and those of previous work in C2C12 myoblasts [11] do not incorporate cell doubling time which is common practice in models such as yeast [37]. We cannot exclude that some proliferation of myoblasts may continue in DM but the low serum conditions and high cell confluency argue against an effect of proliferation substantially inflating protein FSR values particularly during early differentiation. Our FSR data align well with the limited existing literature reporting either average FSR of protein mixtures [11] or protein-specific FSR data [9] [38] in C2C12. Future studies with higher temporal resolution will be required to clarify whether some proliferation continues in the hours immediately after cells are transferred to DM.

FSR data report synthesis as a fraction of an unknown whole (i.e. protein abundance), whereas our current MSR data incorporate FSR measurements with protein-specific abundance data. Linear regression analyses found FSR was a minor component in the variance of MSR during either early or later differentiation (Figure 3A and B, respectively). Therefore, protein abundance was the principal contributing factor to the variance in MSR data, which underpins the advantage of using MSR to investigate experimental scenarios where changes in abundance are expected to co-occur alongside changes in synthesis rates. Indeed, the relationship between data during early and late differentiation improved from r^2=0.19 (FSR; Figure 3C) to r^2=0.73 for (MSR; Figure 3D), which suggests MSR may offer a greater predictive power than fractional data. Protein FSR during early differentiation also had no relationship (r^2=0.04) with protein abundance during later differentiation (Figure 4A). In contrast, protein MSR during early differentiation predicated 78 % of the variance in protein abundance at the later stage of differentiation (Figure 4B). The remaining variance is likely to be accounted for by degradation, which also contributes to both increases and decreases in the abundance of individual proteins [14]. We also compared changes in mRNA expression measured by ribosomal profiling [25] against changes in protein synthesis rates during myoblast differentiation. The relationship between changes in protein synthesis and ribosomal profiling was greater when protein synthesis data was expressed in mole units (Figure 4D, r^2=0.29) rather than fractional terms (Figure 4C, r^2=0.11). Moreover,

a number of disparities (e.g. nestin (NEST), DESM, FLNC and MYH3) between responses reported by ribosomal profiling and protein synthesis measurements were resolved when protein synthesis data were expressed in mole rather than fractional units.

MSR data generated more coherent protein interaction networks than FSR (Figure 5) and the biological interpretation of the data was different when synthesis was expressed in either fractional terms (Figure 5A and C) or mole units (Figure 5B and D). Functional annotation of the top-ranked proteins by MSR found glycolytic processes were enriched during both early (Figure 5B) and late (Figure 5D) differentiation, which was not evident in the analysis of FSR data (Figure 5A and C). In addition, intermediate filament organisation and myofilament protein binding were enriched amongst MSR data during later differentiation. Myofibrillogenesis requires the co-ordinated synthesis of actin, myosin, tropomyosin and alpha actin [6] and, in the current work, myoblast differentiation resulted in significant increases in the abundance of sarcomeric proteins including, embryonic myosin heavy chain (MYH3), essential myosin light chain (MYL1) and the fast-twitch isoform of the sarco-/endoplasmic Ca^{2+} ATPase (AT2A1). Intermediate filament proteins, including desmin (DESM) and vimentin (VIM) were incorporated within the MSR protein networks but were not included in the protein interaction network generated from FSR data (Figure 5B). Furthermore, we detected increases in non-muscle isoforms (MYH9, ML12B), which is consistent with the formation of pre-myofibrils during 72-96 h rather than mature sarcomeres [41].

To the best of our knowledge, we report the first investigation of myoblast differentiation using protein-specific synthesis and abundance measurements in mole rather than fractional units. Our analysis of 115 proteins that met stringent quality control criteria is limited compared to the breadth of analysis of dynamic SILAC, which used higher resolution MS and reported half-life data for 3,528 proteins in C2C12 myotubes only [9]. We anticipate high-resolution MS analysis of deuterium-labelled samples would achieve a similar proteome coverage to dynamic SILAC and biosynthetic labelling with deuterium may afford a greater sensitivity to detect differences in protein synthesis rates. Dynamic SILAC experiments typically monitor the incorporation of heavy isotope at a single lysine or arginine residue

per peptide, whereas deuterium may be incorporated in to the majority of amino acids [22] and could provide a proportionally greater MS signal. Whether deuterium outperforms dynamic SILAC as sample complexity increases remains to be investigated and each approach suffers potentially greater risk of being confounded by co-eluting peptides (e.g. compared to standard label-free quantitation) as sample complexity rises. Deuterium oxide is considerably cheaper than SILAC reagents and can be used in a broader range of biological systems, including humans [14] [15] and rats [12, 21]. Herein, we demonstrate the advantages of combining deuterium labelling with methods [20] for estimating protein abundance in mole units to provide MSR data. Dynamic proteome profiling is a robust method [15] and future application on higher resolution instrumentation is likely to provide more comprehensive data. Currently, it is unclear whether some proteins may be synthesised in excess [9] or whether there are close relationships between protein synthesis and abundance [38]. In addition to investigating cooccurring changes in protein synthesis and abundance, the future use of MSR rather than FSR may allow for new insight by linking changes in ABD to synthesis rates and give a clearer indication of the stoichiometry of multi-protein complexes.

In conclusion, the distribution and biological interpretation of protein synthesis data is different when data are expressed as mole synthesis rate (MSR) rather than fractional synthesis rate (FSR). Proteins of low abundance may be ranked amongst the highest in FSR. Therefore, estimation of MSR provides additional insight in experiments where adaptation involves changes to both the abundance and synthesis rate of proteins. In addition, MSR facilitates investigation of changes to the allocation of cellular resources and an indication of which proteins are being synthesised to the greatest extent. Mole synthesis data is largely unreported but as dynamic proteome profiling methods continue to evolve there is potential to gain additional mechanistic insight using MSR measurements. Mole synthesis data may provide new insight to disparities between mRNA and protein abundance measurements as well as support or dispel theories regarding whether components of multi-protein complexes are synthesised in excess.

4. Conflict of interest statement

The authors have declared no conflict of interest.

References

[1] S. M. Abmayr, G. K. Pavlath, Development 2012, 139, 641.

[2] R. M. Crameri, H. Langberg, P. Magnusson, C. H. Jensen, H. D. Schrøder, J. L. Olesen, C. Suetta, B. Teisner, M. Kjaer, J Physiol 2004, 558, 333.

[3] C. K. Smith, 2nd, M. J. Janney, R. E. Allen, J Cell Physiol 1994, 159, 379.

[4] F. Relaix, P. S. Zammit, Development 2012, 139, 2845.

[5] T. Kislinger, A. O. Gramolini, Y. Pan, K. Rahman, D. H. MacLennan, A. Emili, Mol Cell Proteomics 2005, 4, 887.

[6] R. B. Devlin, C. P. Emerson, Jr., Cell 1978, 13, 599.

[7] N. S. Tannu, V. K. Rao, R. M. Chaudhary, F. Giorgianni, A. E. Saeed, Y. Gao, R. Raghow, Mol Cell Proteomics 2004, 3, 1065.

[8] A. F. Millan-Cubillo, M. Martin-Perez, A. Ibarz, J. Fernandez-Borras, J. Gutierrez, J. Blasco, Sci Rep 2019, 9, 14126.

[9] S. B. Cambridge, F. Gnad, C. Nguyen, J. L. Bermejo, M. Kruger, M. Mann, J Proteome Res 2011, 10, 5275.

[10] B. F. Miller, C. A. Wolff, F. F. Peelor, 3rd, P. D. Shipman, K. L. Hamilton, J Appl Physiol (1985) 2015, 118, 655.

[11] V. C. Foletta, M. Palmieri, J. Kloehn, S. Mason, S. F. Previs, M. J. McConville, O. M. Sieber, C. R. Bruce, G. M. Kowalski, Metabolites 2016, 6.

[12] S. Hesketh, K. Srisawat, H. Sutherland, J. Jarvis, J. Burniston, Proteomes 2016, 4, 12.

[13] S. J. Hesketh, H. Sutherland, P. J. Lisboa, J. C. Jarvis, J. G. Burniston, The FASEB Journal 2020, n/a.

[14] D. M. Camera, J. G. Burniston, M. A. Pogson, W. J. Smiles, J. A. Hawley, Faseb j 2017, 31, 5478.

[15] K. Srisawat, K. Hesketh, M. Cocks, J. Strauss, B. J. Edwards, P. J. Lisboa, S. Shepherd, J. G. Burniston, PROTEOMICS 2019, n/a, 1900194.

[16] J. G. Burniston, Y.-W. Chen, *Omics Approaches to Understanding Muscle Biology*, Springer, 2019.

[17] L. Li, C. J. Nelson, C. Solheim, J. Whelan, A. H. Millar, Molecular & cellular proteomics : MCP 2012, 11, M111.010025.

[18] C. Gerner, S. Vejda, D. Gelbmann, E. Bayer, J. Gotzmann, R. Schulte-Hermann, W. Mikulits, Molecular & cellular proteomics : MCP 2002, 1, 528.

[19] K. J. Sollanek, J. G. Burniston, A. N. Kavazis, A. B. Morton, M. P. Wiggs, B. Ahn, A. J. Smuder, S. K. Powers, PloS one 2017, 12, e0171007; Z. A. Malik, J. N. Cobley, J. P. Morton, G. L. Close, B. J. Edwards, L. G. Koch, S. L. Britton, J. G. Burniston, Proteomes 2013, 1, 290; J. G. Burniston, J. Connolly, H. Kainulainen, S. L. Britton, L. G. Koch, PROTEOMICS 2014, 14, 2339.

[20] J. C. Silva, M. V. Gorenstein, G. Z. Li, J. P. Vissers, S. J. Geromanos, Mol Cell Proteomics 2006, 5, 144.

[21] C. A. Stead, S. J. Hesketh, S. Bennett, H. Sutherland, J. C. Jarvis, P. J. Lisboa, J. G. Burniston, Proteomes 2020, 8.

[22] A. J. Holmes, P. J. Rayner, M. J. Cowley, G. G. R. Green, A. C. Whitwood, S. B. Duckett, Dalton Trans 2015, 44, 1077.

[23] J. D. Storey, R. Tibshirani, Proceedings of the National Academy of Sciences 2003, 100, 9440.

[24] J. Cox, M. Mann, BMC Bioinformatics 2012, 13 Suppl 16, S12.

[25] E. de Klerk, I. F. Fokkema, K. A. Thiadens, J. J. Goeman, M. Palmblad, J. T. den Dunnen, M. von Lindern, P. A. t Hoen, Nucleic Acids Res 2015, 43, 4408.

[26] S. Tyanova, T. Temu, P. Sinitcyn, A. Carlson, M. Y. Hein, T. Geiger, M. Mann, J. Cox, Nature Methods 2016, 13, 731.

[27] D. Szklarczyk, A. L. Gable, D. Lyon, A. Junge, S. Wyder, J. Huerta-Cepas, M. Simonovic, N. T. Doncheva, J. H. Morris, P. Bork, L. J. Jensen, C. V. Mering, Nucleic Acids Res 2019, 47, D607.

[28] A. Harada, Y. Ohkawa, A. N. Imbalzano, Semin Cell Dev Biol 2017, 72, 77.
[29] K. A. Carey, D. Segal, R. Klein, A. Sanigorski, K. Walder, G. R. Collier, D. Cameron-Smith, Pathology International 2006, 56, 246.
[30] S. Kumari, S. Roy, P. Singh, S. L. Singla-Pareek, A. Pareek, Plant Signal Behav 2013, 8, e22734.
[31] S. K. Calderwood, A. Murshid, T. Prince, Gerontology 2009, 55, 550.
[32] N. Khurana, S. Bhattacharyya, Front Oncol 2015, 5, 100.
[33] Y. Feng, Z.-M. Tian, M.-X. Wan, Z.-B. Zheng, World J Gastroenterol 2007, 13, 2608.
[34] L. Liu, T. H. Cheung, G. W. Charville, B. M. Hurgo, T. Leavitt, J. Shih, A. Brunet, T. A. Rando, Cell Rep 2013, 4, 189.
[35] A. Fathi, M. Pakzad, A. Taei, T. C. Brink, L. Pirhaji, G. Ruiz, M. Sharif Tabe Bordbar, H. Gourabi, J. Adjaye, H. Baharvand, G. Hosseini Salekdeh, PROTEOMICS 2009, 9, 4859.
[36] V. Andrés, K. Walsh, J Cell Biol 1996, 132, 657.
[37] M. Martin-Perez, J. Villén, Cell Syst 2017, 5, 283.
[38] A. R. Kristensen, J. Gsponer, L. J. Foster, Mol Syst Biol 2013, 9, 689.
[39] S. E. Kruse, P. P. Karunadharma, N. Basisty, R. Johnson, R. P. Beyer, M. J. MacCoss, P. S. Rabinovitch, D. J. Marcinek, Aging Cell 2016, 15, 89.
[40] D. E. Hammond, A. J. Claydon, D. M. Simpson, D. Edward, P. Stockley, J. L. Hurst, R. J. Beynon, Mol Cell Proteomics 2016, 15, 1204.
[41] J. W. Sanger, P. Chowrashi, N. C. Shaner, S. Spalthoff, J. Wang, N. L. Freeman, J. M. Sanger, Clin Orthop Relat Res 2002, S153.

Figure Legends

Figure 1 – C2C12 morphology and mass spectra at different stages of differentiation.

Representative light micrograph images of undifferentiated C2C12 myoblasts (0 h; A), and multinucleated myotubes grown without (96 H_2O; B) or with (96 h D_2O; C) heavy isotope label. Density plots of myotube length (D), diameter (E) and area (F) at 96 h in control (red) and labelled (blue) cultures. Mass spectra of peptide $[M+2H]^{2+}$ 894.4711 *m/z* TITLEVEPSDTIENVK (residues 12-27) of ubiquitin-40S ribosomal protein S27a (RS27A) from undifferentiated C2C12 myoblasts (0 h; G), and multinucleated myotubes grown without (96 H_2O; H) or with (96 h D_2O; I) heavy isotope label. Changes in the fraction of the monoisotopic peak (fm_0) were used to calculate synthesis rates (see Equation 2).

Figure 2 – Protein abundance changes during differentiation.

(A) Volcano plot illustrating Log2 fold-change in protein abundance in late (72-96 h) compared to early (0-24 h) differentiation. Statistically significance was determined by one-way ANOVA (153 proteins in n=3 samples per group). Data points situated to the left and right of the Y axis represent proteins with a greater abundance in either early or late differentiation, respectively. Proteins exhibiting significant ($P<0.05$, FDR < 1%) differences are coloured red and labelled by their UniProt ID. (B) 2D Enrichment [24] analysis of significant ($P<0.02$) biological process (red), cellular component (green) and molecular function (blue) annotations in the current protein abundance data (n=107) that matched with RNA sequencing data reported in de Klerk et al [25]. (C) Linear regression of protein abundance change and gene expression change data (n=107) used to build the 2D enrichment plot. Consistent with (A) positive

fold-change values represent a greater protein abundance/ mRNA expression in late compared to early differentiation.

Figure 3 – Comparison of mole and fractional synthesis data in C2C12 cells

Linear regression analysis (n=115 proteins) of FSR (%/h) and MSR (fmol/h/ug total protein) during early (0-24 h; A) and late (72-96 h; B) differentiation. Differences between early (0-24 h) and late (72-96 h) differentiation in FSR (C) and MSR (D). Labels represent UniProt identifiers.

Figure 4 – Predictive value of FSR and MSR data

Linear regression of protein abundance during late differentiation and either FSR (A) or MSR (B) during early (0-24 h) differentiation (n=115 proteins). Linear regression of the change in either FSR (C) or MSR (D) during late versus early differentiation against ribosomal profiling data reported in de Klerk et al [25]. Positive fold-change values represent greater synthesis in late compared to early differentiation and data points of interest are labelled by their UniProt identifier.

Figure 5 – Protein-protein interaction networks

Protein-protein interaction networks derived from the top 10 proteins ranked by either FSR (A and C) or MSR (B and D) during either early (A and B) or late (C and D) differentiation. Networks were constructed using the search tool for the retrieval of interacting genes/proteins (STRING). Interaction confidence criteria was set to medium (0.4). Nodes are labelled by gene names and line thickness represents the strength of the data supporting each interaction.

418 Figure 1

419

420

421

Figure 1

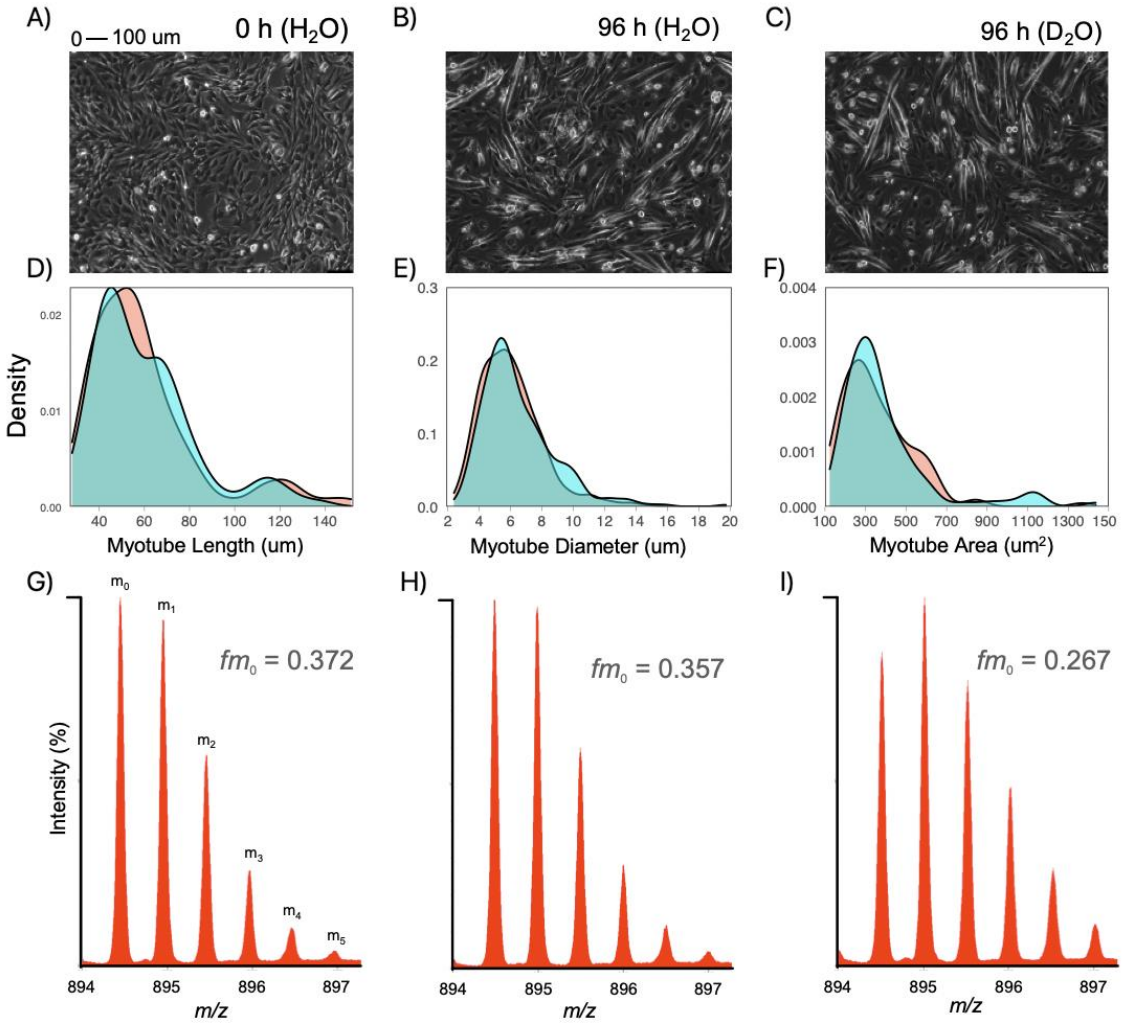
A)
0 — 100 um
0 h (H_2O)
B)
96 h (H_2O)
C)
96 h (D_2O)
D)
Density
Myotube Length (um)
E)
Myotube Diameter (um)
F)
Myotube Area (um²)
G)
m_0
m_1
m_2
m_3
m_4
m_5
fm_0 = 0.372
Intensity (%)
m/z
H)
fm_0 = 0.357
m/z
I)
fm_0 = 0.267
m/z

427 Figure 2

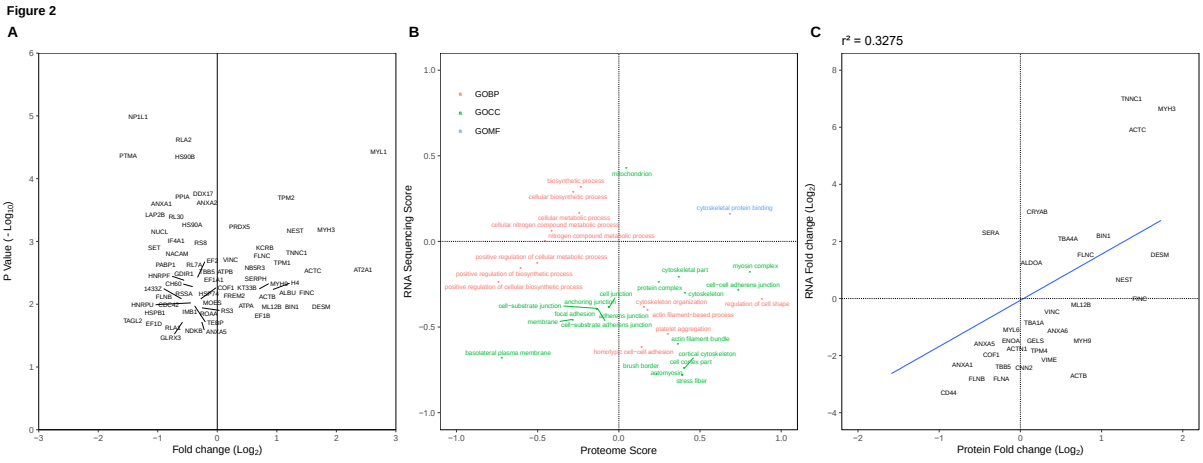

428

429

430 Figure 3

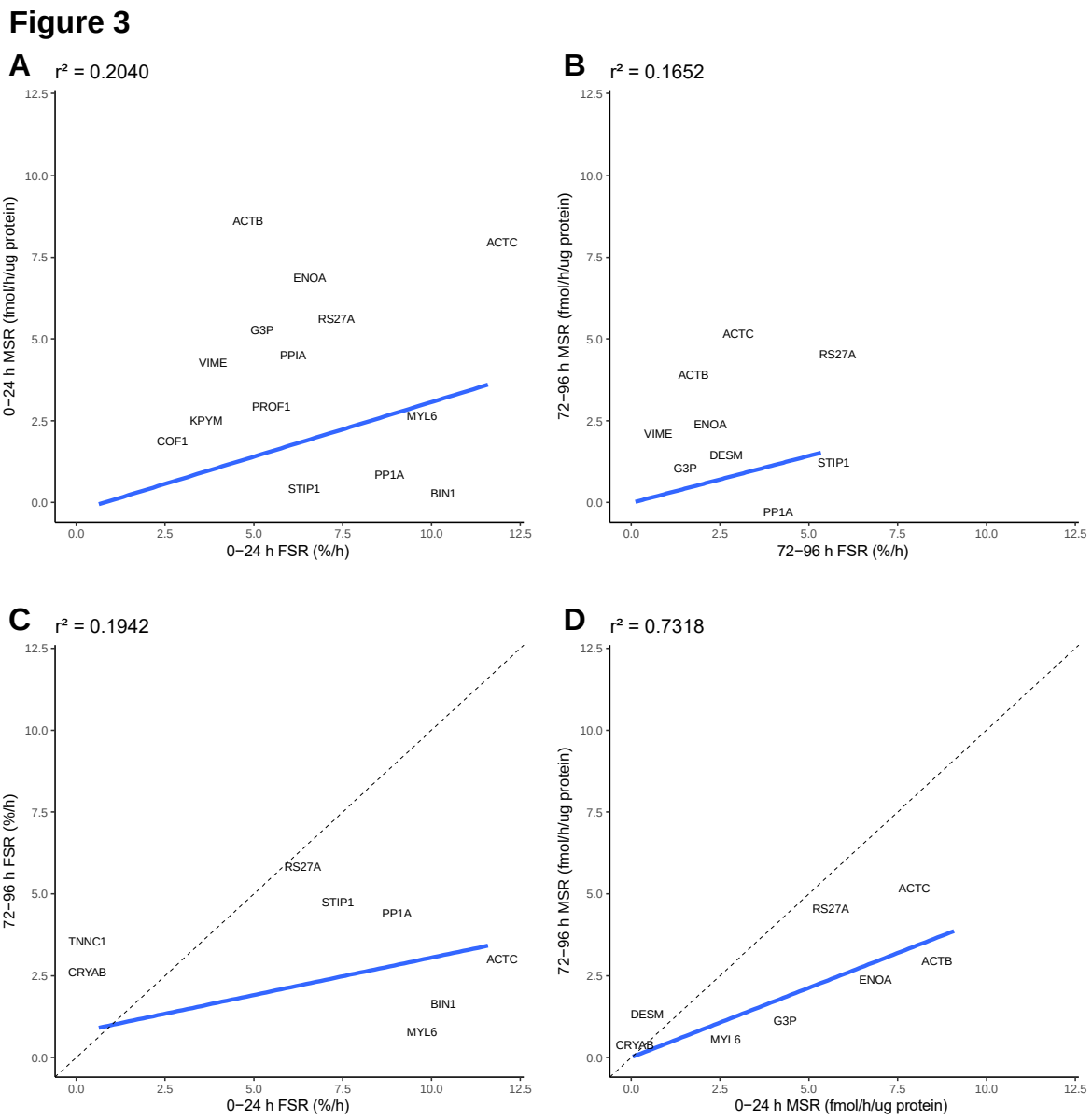

431

432

433 Figure 4

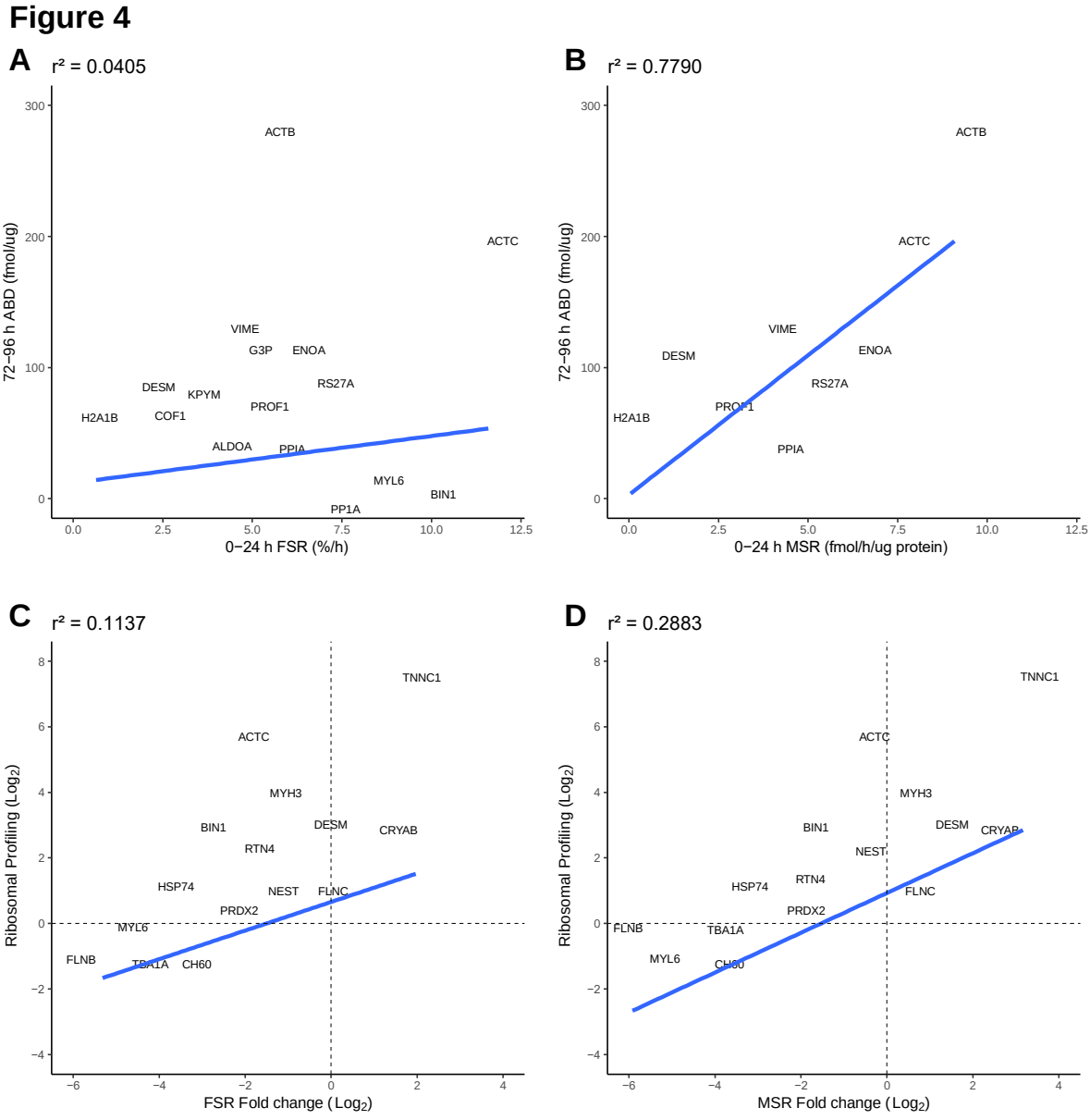

434

435

436

437 Figure 5

Figure 5

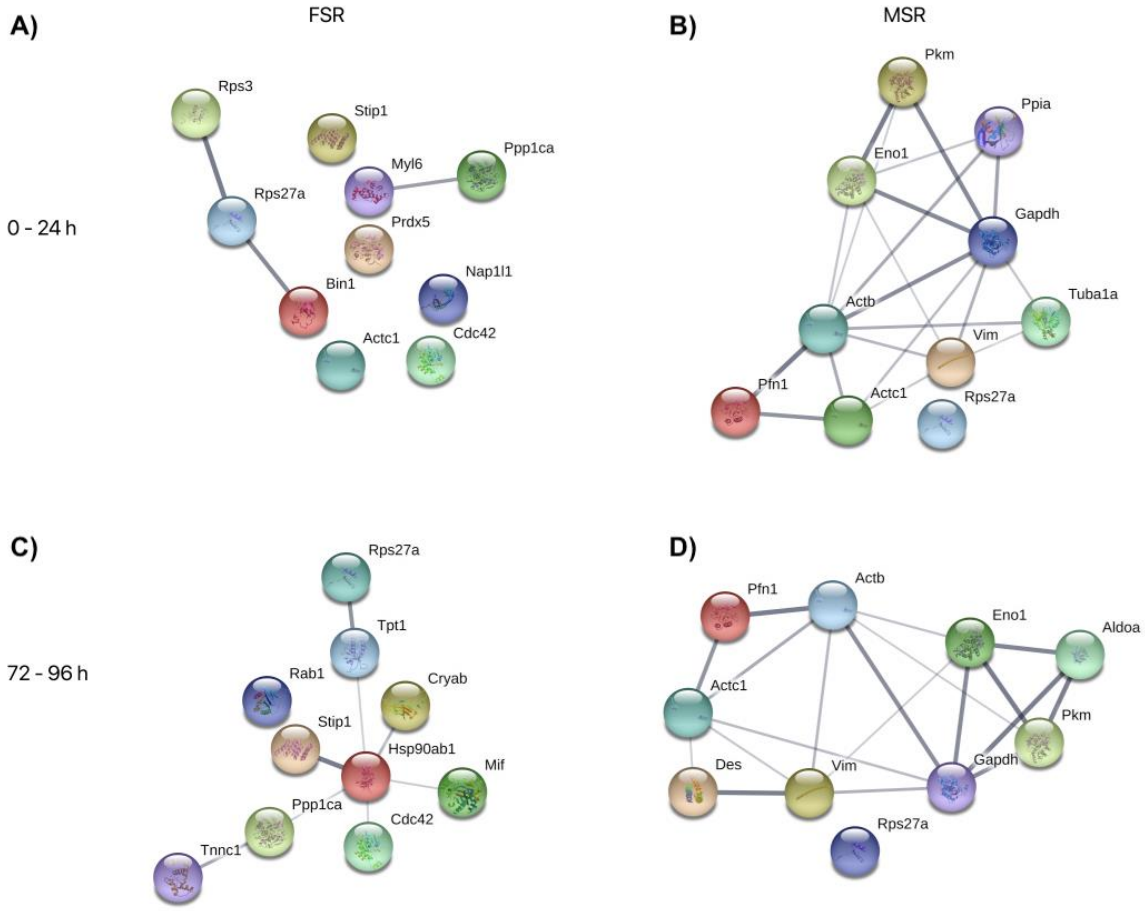

438

439

440